CHAPTER 3

RESULTS & DISCUSSIONS

3.1 PREFORMULATION STUDIES OF ISONIAZID

3.1.1 Identification of drug

3.1.1.1 Physical appearance

Isoniazid was physically examined for organoleptic properties. It was found to be white, odourless, crystalline powder.

Table 3.1 Physical appearance of Isoniazid

S. No.	Characteristics	Observation
1	State	Solid, Crystalline nature
2	Colour	White
3	Odour	Odourless
4	Taste	Bitter

3.1.1.2 Melting Point

The melting point of Isoniazid was found to be 171.5 ±1.5 by thiels tube method.

Table 3.2 Melting Point of Isoniazid

S. No.	Drug	Melting Point (°C)
1	Isoniazid	171.5 ±1.5

Data shown are the mean ± SD (n=3).

3.1.1.3 Solubility studies

The solubility study of Isoniazid was determined in various aqueous and non-aqueous solvents. Isoniazid was soluble in water, slightly soluble in methanol, ethanol and chloroform and very slightly soluble in ether.

3.1.2 ANALYTICAL METHOD DEVELOPMENT FOR ISONIAZID BY UV-VISIBLE SPECTROPHOTOMETER.

UV Spectroscopy method was developed for the analysis of Isoniazid, using double beam Shimadzu 1700 UV spectroscopy.

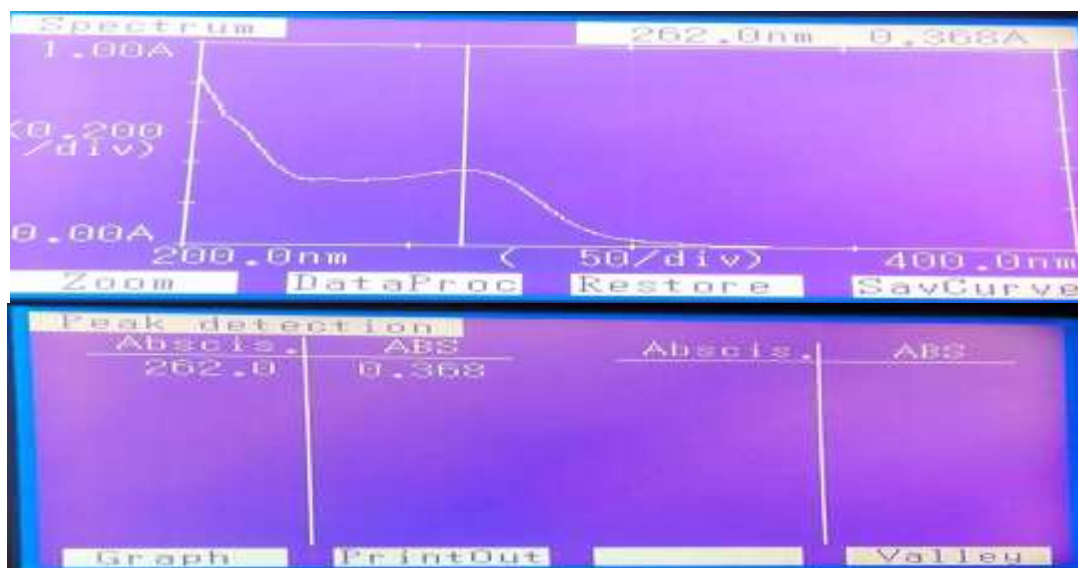### 3.1.2.1 Detertmination of λ_{max} of Isoniazid

Fig 3.1 λ_{max} of Isoniazid

The optimized λ max of Isoniazid was found to be 262nm.

3.1.2.2 Calibration curve of Isoniazid

The absorbance of prepared dilutions (2, 4, 6, 8, 10 µg/ml) were measured by UV-Visible spectrophotometer at its own λ_{max} 262 nm and thereafter at λ_{max} 268.5 nm belonging to PYZ against 7.4 pH phosphate buffer . The absorbance so obtained is tabulated in table and calibration curve was plotted. The regressed data is shown as straight line. The regression coefficient was found to be 0.9995 and 0.9983 indicating good linearity as shown in Fig 3.2 and Fig 3.3. The calibration curve obeyed Beers Lamberts law in the concentration range 2-10 µl.
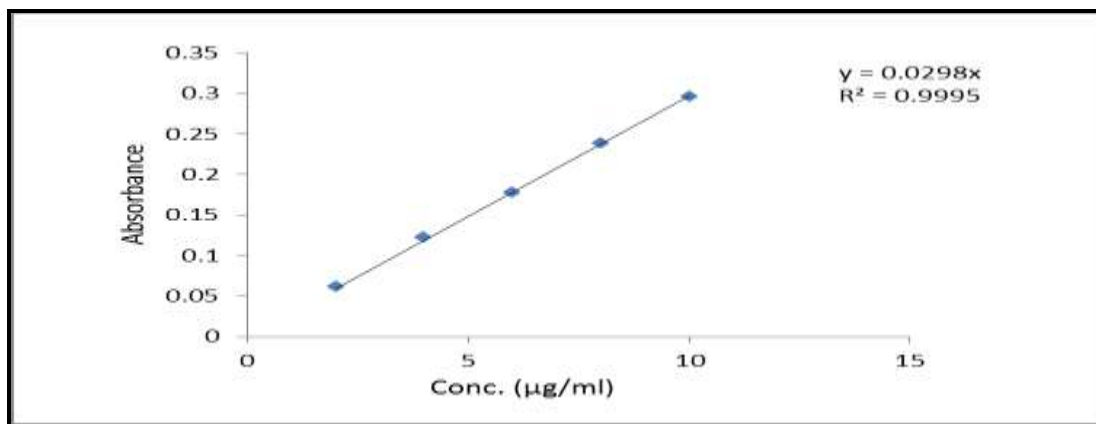

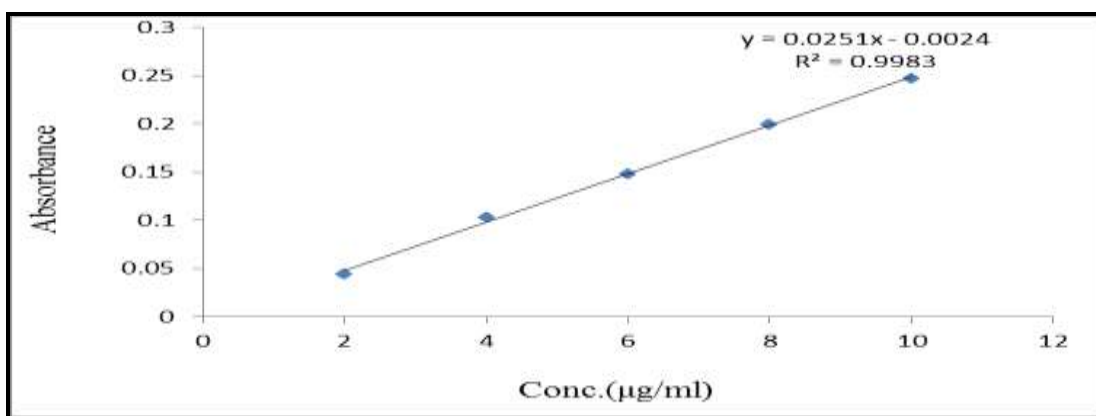**Fig 3.2 Standard curve of Isoniazid at 262nm**

Fig 3.3 Standard curve of Isoniazid at 268.5nm

3.1.3 SPECTRAL ANALYSIS (FTIR) OF ISONIAZID

On comparing the IR spectrum of sample (Isoniazid) and reference spectrum, it was observed that all characteristic peaks of drugs were found as shown in Fig 3.4(b)
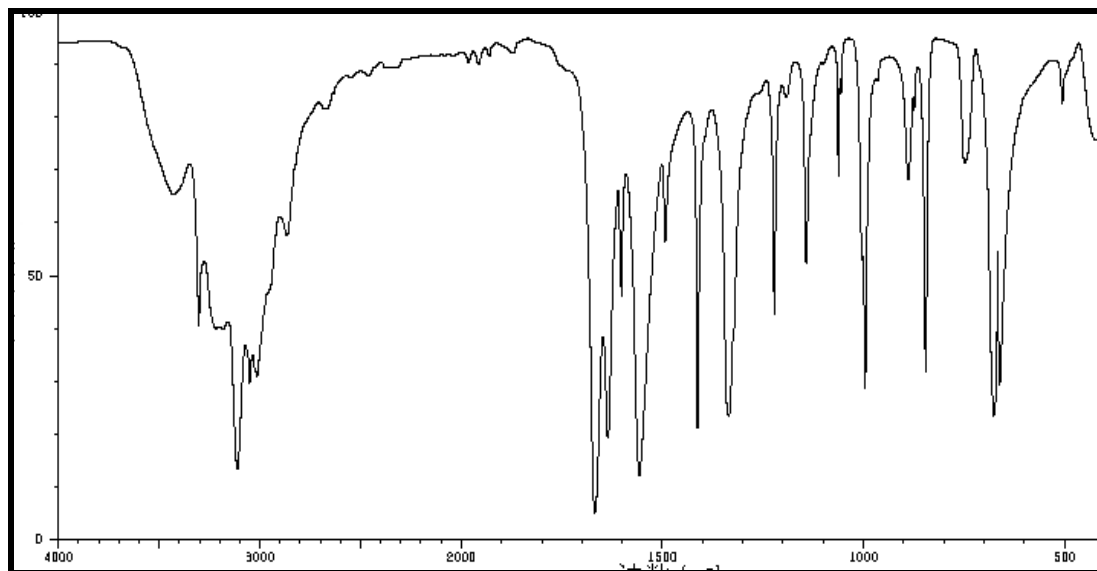

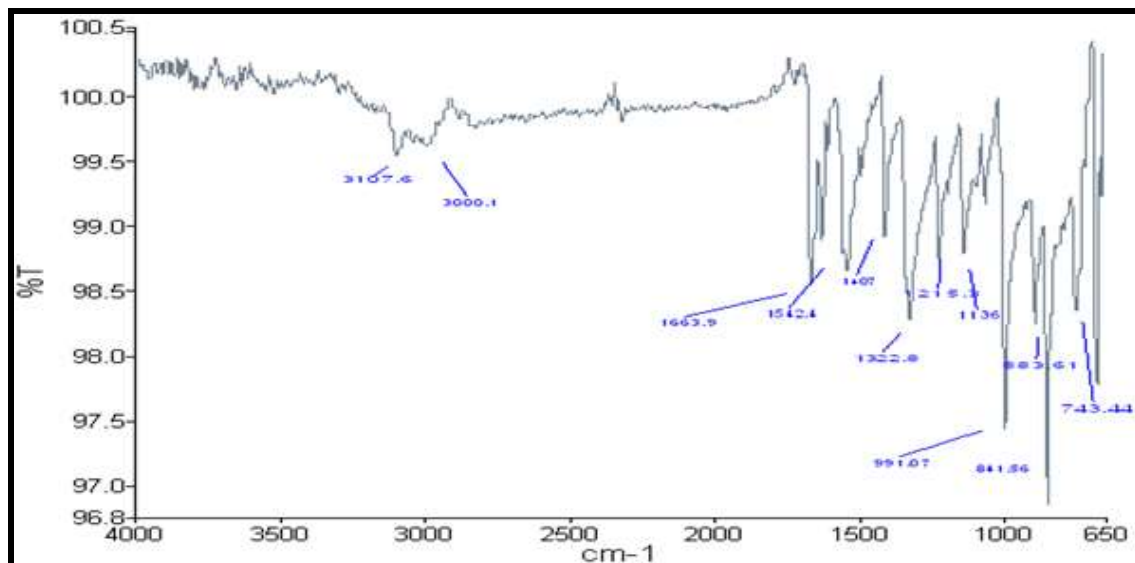**Fig 3.4(a) IR Spectra of Isoniazid(reference)**

Fig 3.4(b) IR Spectra of Isoniazid (Sample)

Table 3.3 IR characterization of Isoniazid

S. No.	Wave no.(cm^{-1})	Vibration mode	May be due to
1.	3000.1	C-H str	Aromatic ring
2.	3107.6	N-H str	Primary amine
3.	1322.8	C=C str	Aromatic ring
4.	1407	C=N str	pyridine ring
5.	1663.9	C=O str	Amide-I
6.	1542.4	N-H bending	Amide-II
7.	841.56	C-H def (oop)	Aromatic ring

3.2 PREFORMULATION STUDIES OF PYRAZINAMIDE

3.2.1 Identification of drug

3.2.1.1 Physical appearance

The Drug sample was studied for its organoleptic properties. The drug was white in colour, odourless, crystalline powder.

Table 3.4 Physical properties of Pyrazinamide

S. No.	Characteristics	Observation
1	State	Solid, Crystalline nature
2	Colour	White
3	Odour	Odourless
4	Taste	Bitter

3.2.1.2 Melting Point

Melting point of Pyrazinamide was found to be 190 ± 1 ^{o}C by thiels tube method.

3.2.1.3 Solubility study

The solubility study of Pyrazinamide was determined in various aqueous and non-aqueous solvents. Pyrazinamide was soluble in water, chloroform, slightly soluble in ethanol, methanol.

3.2.2 ANALYTICAL METHOD DEVELOPMENT FOR PYRAZINAMIDE BY UV – VISIBLE SPECTROPHOTOMETER.

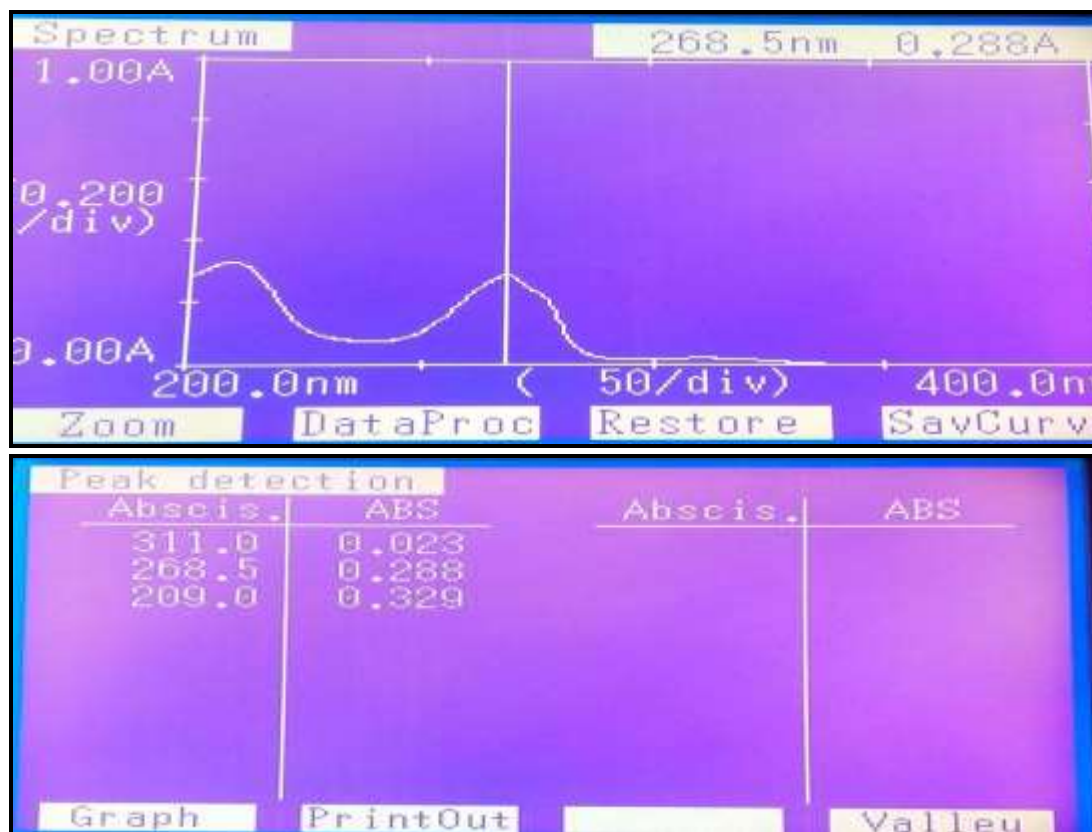### 3.2.2.1 Detertmination of λ_{max} of Pyrazinamide

Fig 3.5 λ_{max} of Pyrazinamide

The optimized λ_{max} of Pyrazinamide was found to be 268.5 nm.

3.2.2.2 Calibration curve of Pyrazinamide

The absorbance of prepared dilutions (2, 4, 6, 8, 10 µg/ml) were measured by UV-Visible spectrophotometer at λ_{max} of PYZ i.e. 268.5 nm and thereafter at λ_{max} 262nm belonging to INH against 7.4 pH buffer. The absorbance so obtained is tabulated in table and calibration curve was plotted. The regressed data showed straight line. The regression coefficient was found to be 0.9995 and 0.9974 respectively, indicating good linearity as shown in Fig 3.6 and Fig 3.7. The calibration curve obeyed Beers Lamberts law in the concentration range 2-10 µl.
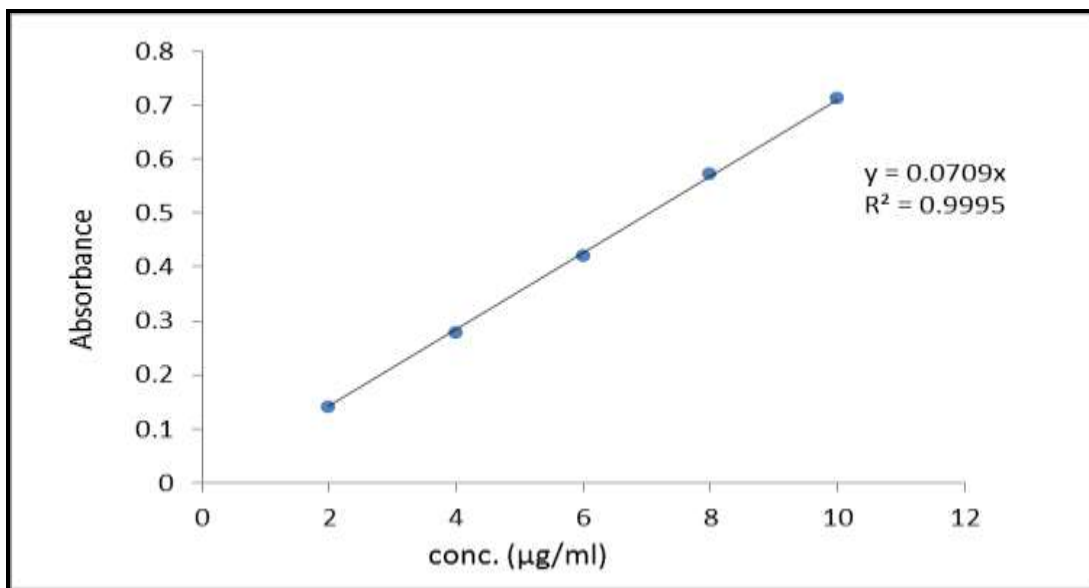

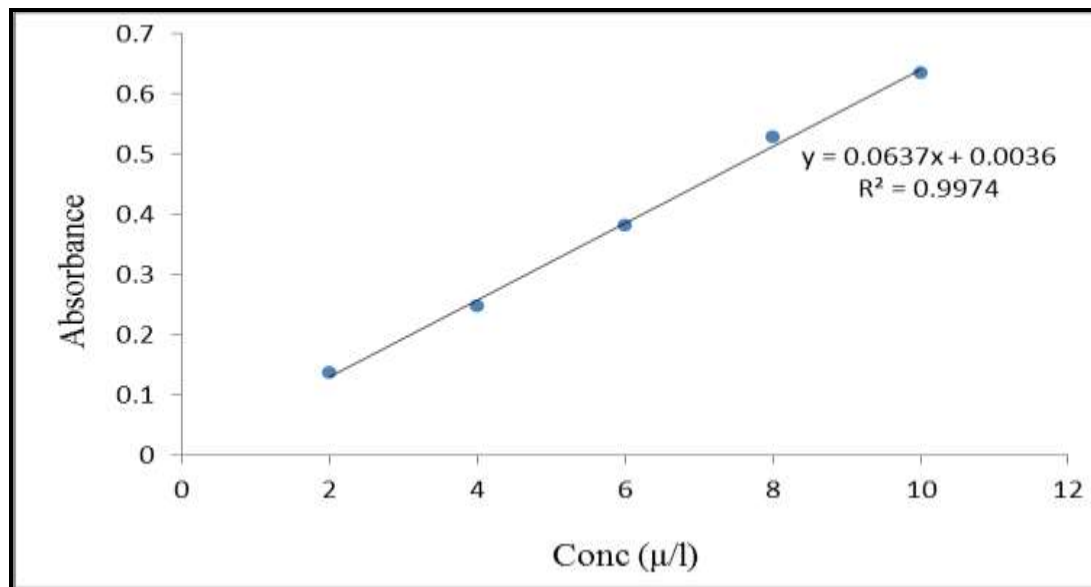**Fig 3.6 Standard curve of Pyrazinamide at 268.5 nm**

Fig 3.7 Standard curve of Pyrazinamide at 262 nm

3.2.3 SPECTRAL (FTIR) ANALYSIS OF PYRAZINAMIDE

On comparing the IR spectrum of sample (Pyrazinamide) and Reference spectrum, it was observed that all characteristic peaks of drugs were found as shown in Fig 3.8(b)
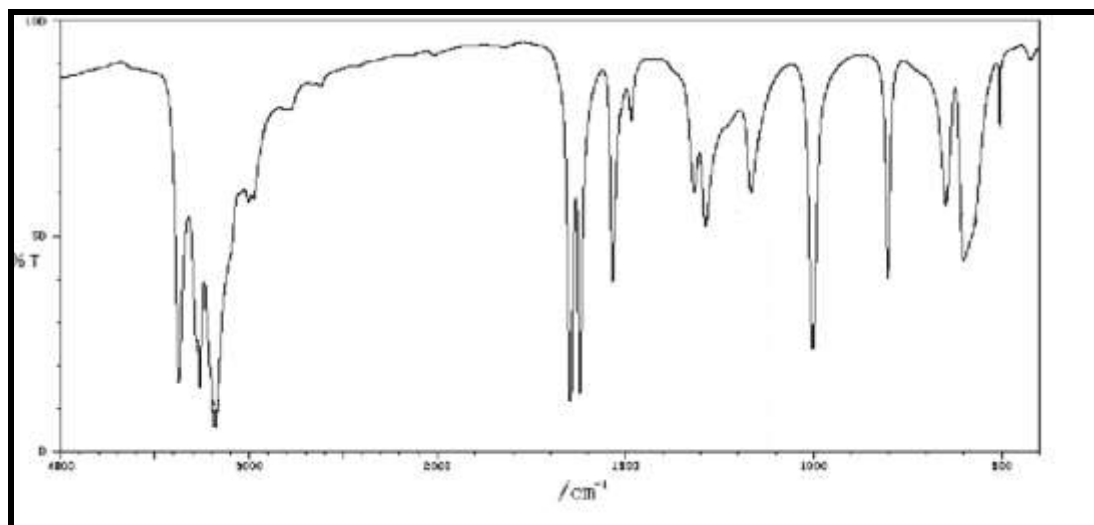
Fig 3.8(a) IR Spectrum of Pyrazinamide (reference)
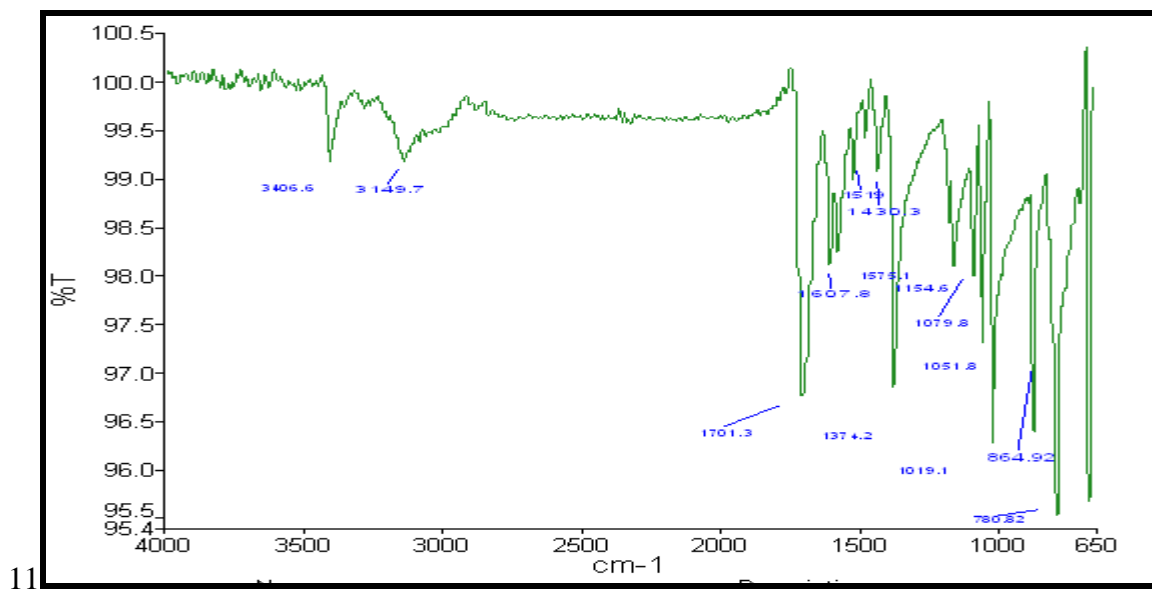
Fig 3.8 (b) IR Spectrum of Pyrazinamide (sample)

Table 3.5 IR characterization of Pyrazinamide

S. No.	Wave no.(cm^{-1})	Vibration mode	Due to
1.	3149.7	C-H str	Aromatic ring
2.	3406.6	N-H str	Primary amine
3.	1519, 1430.3	C=C str	Aromatic ring
4.	1575.1	C=N str	Pyrazine ring
5.	1701.3	C=O str	Amide-I
6.	1607.8	N-H bending	Amide-II
7.	780.82	C-H def (oop)	Aromatic ring

3.3 DRUG EXCIPIENT INTERACTION STUDY

3.3.1 IR spectrum of drugs and polymers (Formulation 1)

The characteristic absorption peaks of Isoniazid, Pyrazinamide were observed in recorded IR spectra of physical mixture containing drugs (INH and PYZ) and excipients (chitosan, sodium tripolyphosphate) used in formulation 1. The FTIR results revealed that there was no interaction between drugs (INH and PYZ) and excipients (chitosan, sodium tripolyphosphate) used in formulation. IR Spectra is shown in Fig 3.9.
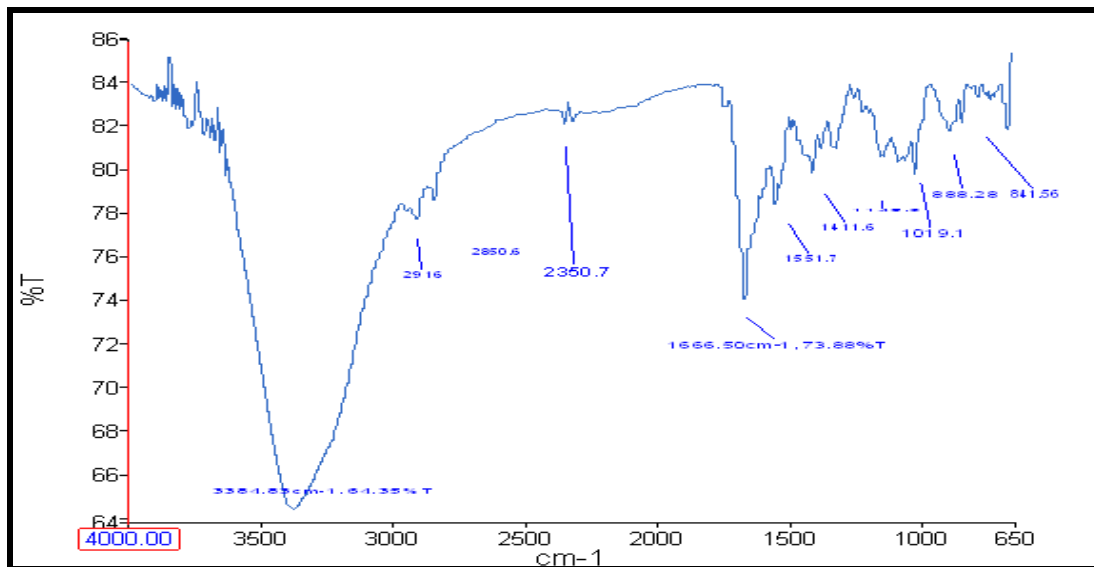
Fig 3.9 IR spectrum of drug polymer interaction (Formulation I)

Table 3.6 IR Characteristics of Drugs and polymer interaction (Formulation 1)

S. No.	Wave no.(cm^{-1})	Vibration mode	Due to
1.	3384.33	N-H str	Primary amine
2.	2916	C-H str	Aromatic ring
3.	2850.6	C-H str	Methyl group
4.	1666.50	C=O str	Amide I
5.	1551.7	N-H ben	Amide-II
6.	1411.6	C=N str	Pyrazine/Pyridine
7.	1019.1	C-O-C ring stre	Pyranose
8.	888.28	C-H def (oop)	Aromatic ring

3.3.1.1 I.R spectrum of drugs, polymers and ligand (D-mannose)

The characteristic absorption peaks of Isoniazid, Pyrazinamide were observed in recorded IR spectra of physical mixture containing drugs (INH and PYZ) and excipients (chitosan, sodium tripolyphosphate, D-mannose) used in formulation 1. The FTIR results revealed that there was no interaction between drugs (INH and PYZ) and excipients (chitosan, sodium tripolyphosphate, D mannose) used in formulation. IR Spectra is shown in Fig 3.10.


Fig 3.10 I.R spectrum of drugs, polymers and ligand (D-mannose) (Formulation I)

Table 3.7 IR Characteristics of Drugs, polymer and ligand (D-mannose) interaction

S. No.	Wave no.(cm $^{-1}$)	Vibration mode	May be due to
1	3410.33	N-H str	Primary amine
2	2920.7	C-H str	Aromatic ring
3	2850.6	C-H str	Methyl group

4	1665.98	C=O str	Amide I
5	1411.6	N-H bending	Amide II
6	1271.4	C=N str	Pyrazine/Pyridine
7	1023.8	C-O-C ring str	Pyranose

3.3.1.2 I.R spectrum of drugs, polymers and ligand (Folic acid)

The characteristic absorption peaks of Isoniazid, Pyrazinamide were observed in recorded IR spectra of physical mixture containing drugs (INH and PYZ) and excipients (chitosan, sodium tripolyphosphate, Folic acid) used in formulation 1. The FTIR results revealed that there was no interaction between drugs (INH and PYZ) and excipients (chitosan, sodium tripolyphosphate and folic acid) used in formulation. IR Spectra is shown in Fig 3.11.
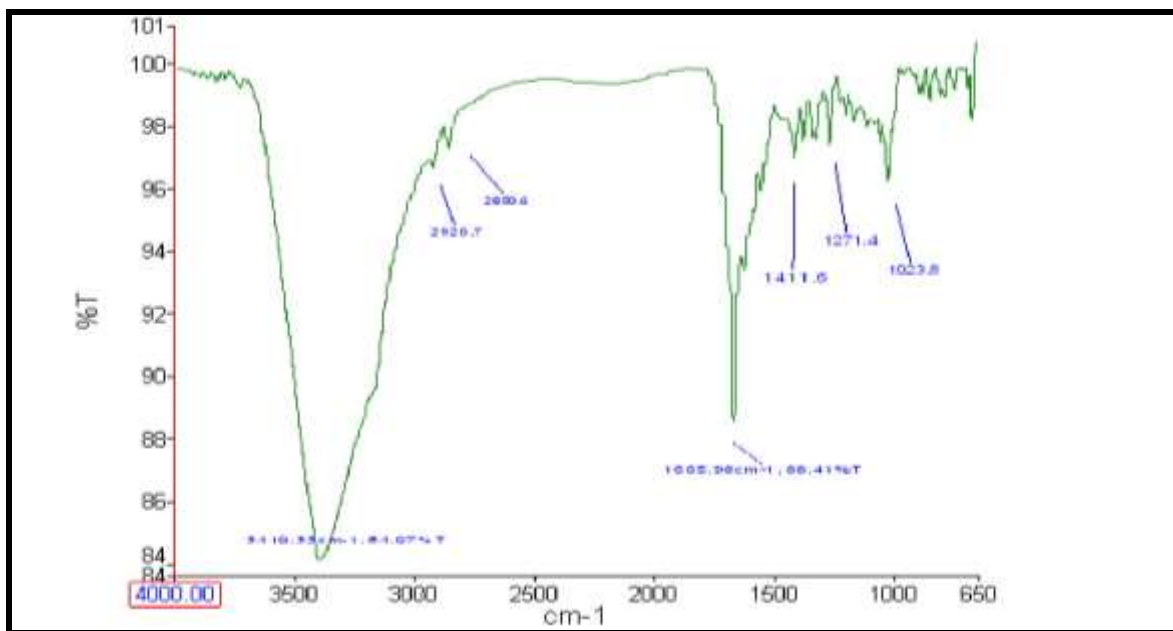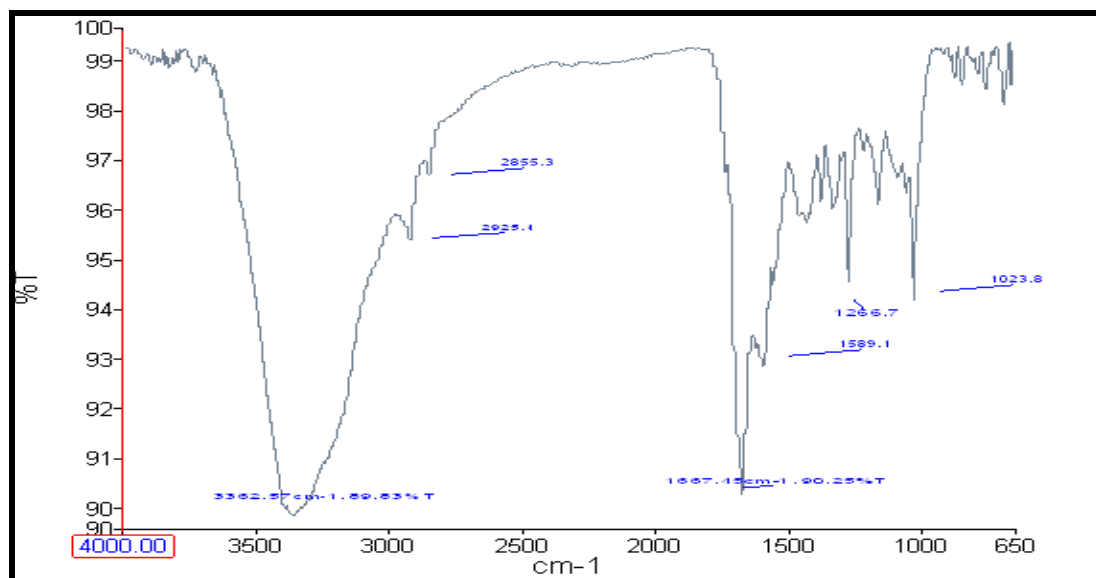

Fig 3.11 I.R spectrum of drugs, polymers and ligand (Folic acid)

Table 3.8 IR Characteristics of Drugs, polymer and ligand (Folic acid) interaction

S.No.	Wave no.(cm^{-1})	Vibration mode	May be due to
1	3362.57	N-H stre	Primary amine
2	2925.4	C-H stre	Aromatic ring
3	2855.3	C-H stre	Methyl group
4	1667.45	C=O str	Amide I
5	1589.1	N-H bending	Amide II
6	1266.7	C=N str	Pyrazine/Pyridine
7	1023.8	C-O-C ring str	Pyranose

3.3.2 IR spectrum of drugs and polymers (Formulation 2)

The characteristic absorption peaks of Isoniazid and Pyrazinamide were observed in recorded IR spectra of physical mixture containing drugs (INH and PYZ) and excipients (chitosan, sodium alginate and calcium chloride)used in formulation 2. The FTIR results revealed that there was no interaction between drugs (INH and PYZ) and excipients (sodium alginate, chitosan, calcium chloride) used in formulation. IR Spectra is shown in Fig 3.12.

Fig 3.12 IR spectrum of drug polymer interaction (Formulation 2)

Table 3.9 IR Characteristics of Drugs and polymer interaction (Formulation 2)

S. No.	Wave no. (cm^{-1})	Vibration mode	Due to
1.	3414.34	N-H str (asym)	Primary amine
2.	3285.23	N-H str (sym)	Primary amine
3.	3174.51	C-H str	Aromatic ring
4.	1714.20	C=O str	Amide I
5.	1666.84	N-H bend	Amide-II
6.	1613.70	C=N str	Pyrazine /Pyridine
7.	1479.41,1378.83	C=C ring str	Aromatic ring
8.	786.5	C-H bend (oop)	Aromatic ring

3.3.2.1 I.R spectrum of drugs, polymers and ligand (D-mannose)

The characteristic absorption peaks of Isoniazid and Pyrazinamide were observed in recorded IR spectra of physical mixture containing drugs (INH and PYZ) and excipients (sodium

alginate, chitosan, calcium chloride, D-mannose) used in formulation 2. The FTIR results revealed that there was no interaction between drugs (INH and PYZ) and excipients (sodium alginate, chitosan, calcium chloride, D-mannose) used in formulation2. IR Spectra is shown in Fig 3.13
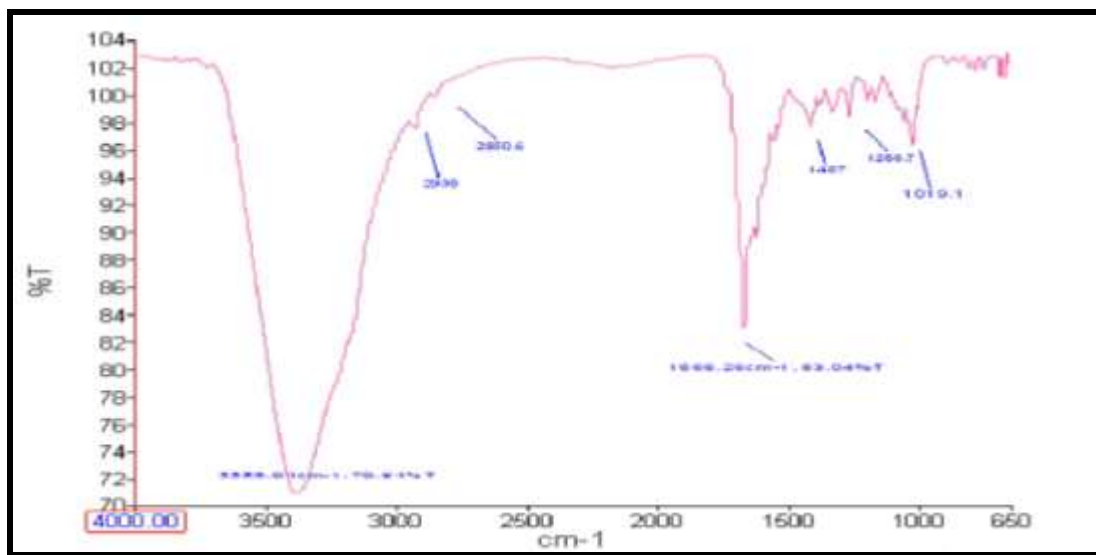

Fig 3.13 I.R spectrum of drugs, polymers and ligand (D-mannose)

Table 3.10 IR Characteristics of drugs, polymers and ligand (D-mannose) interaction

S.No.	Wave no.(cm $^{-1}$)	Vibration mode	May be due to
1	3388.01	N-H str	Primary amine
2	2930	C-H str	Aromatic ring
3	2850.6	C-H str	Methyl group
4	1666.26	C=O str	Amide I
5	1407	N-H bending	Amide II
6	1266.7	C=N str	Pyrazine/Pyridine
7	1019.1	C-O-C ring str	Pyranose

3.3.2.2 I.R spectrum of drugs, polymers and ligand (Folic acid)

The characteristic absorption peaks of Isoniazid and Pyrazinamide were observed in recorded IR spectra (sodium alginate, chitosan, calcium chloride, folic acid) used in formulation 2. The FTIR results revealed that there was no interaction between drugs (INH and PYZ) and excipients (sodium alginate, chitosan, calcium chloride, folic acid) used in formulation 2. IR Spectra is shown in Fig 3.14.
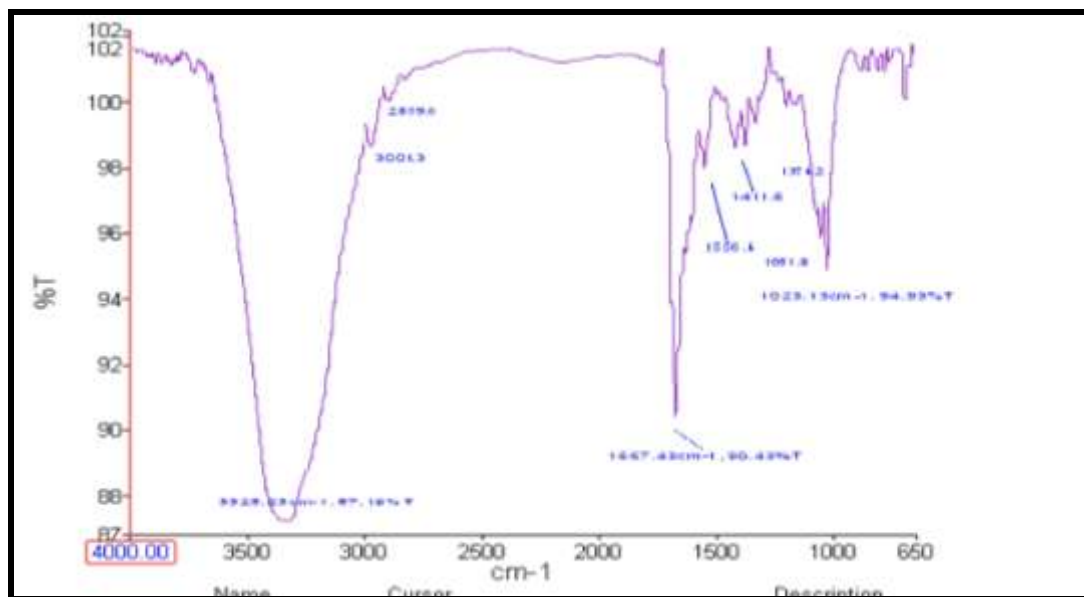

Fig 3.14 I.R spectrum of drugs, polymers and ligand (Folic acid)

Table 3.11 IR Characteristics of drugs, polymers and ligand (Folic acid) interaction

S.No.	Wave no.(cm^{-1})	Vibration mode	Due to
1	3325.23	N-H str	Primary amine
2	3001.3	C-H str	Aromatic ring
3	2859.6	C-H str	Methyl group
4	1667	C=O str	Amide I

5	1556.4	N-H bending	Amide II
6	1411.6	C=N str	Pyrazine/Pyridine
7	1023.13	C-O-C ring str	Pyranose

3.4 SELECTION OF ANALYTICAL WAVELENGTH FOR SIMULTANEOUS ESTIMATION OF DRUGS

3.4.1 Overlay spectrum of Isoniazid and Pyrazinamide for simultaneous estimation of drugs.

In overlay spectrum, individual spectra of isoniazid and pyrazinamide were overlapped to find all points of intersection. The observed intersection points in overlay spectrum were at 225nm, 252 nm, 283.5 nm with absorbance 0.160A, 0.165 A and 0.078 A as shown in table 3.12. The highest intersection point was considered as isobestic point for analysis of drugs in combined formulation.
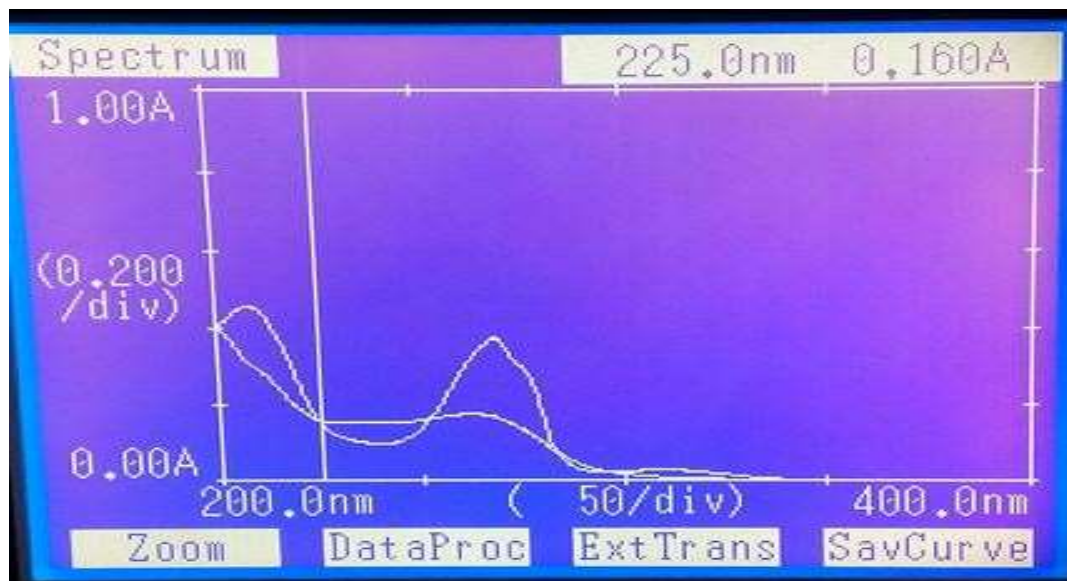

Fig 3.15 Overlay spectra of INH and PYZ with intersection point 225 nm
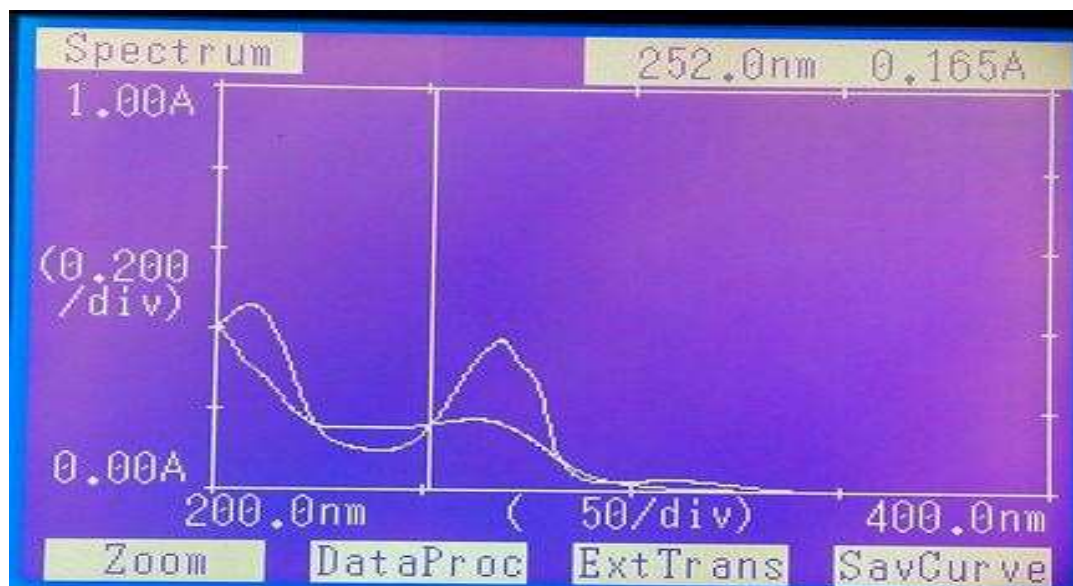
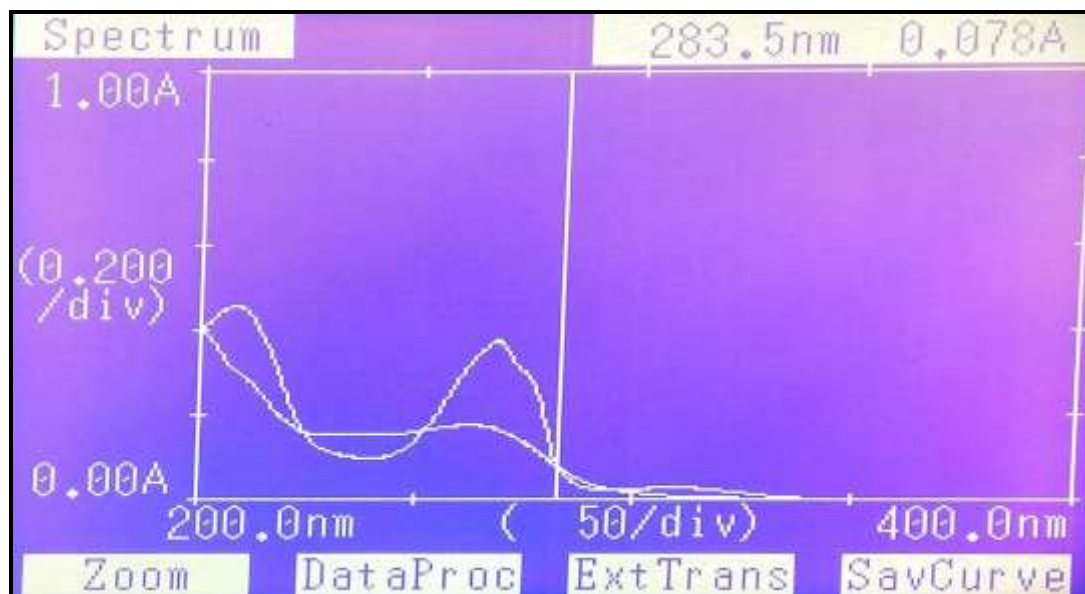**Fig 3.16 Overlay spectra of INH and PYZ with intersection point 252nm**

Fig 3.17 Overlay spectra of INH and PYZ with intersection point 283.5nm

Table 3.12 Isobestic Point Determination

Intersecting Points	Ist	IInd	IIIrd	Isobestic Point
λ_{max} (nm)	225	252	283.5	252
Absorbance	0.160	0.165	0.078	0.165

λ_{max} (Isobestic Point) for simultaneous estimation of Pyrazinamide and Isoniazid was found to be 252nm.

3.5 CHARACTERIZATION AND EVALUATION OF CHITOSAN NANOPARTICLES

Isoniazid and Pyrazinamide loaded chitosan nanoparticles were prepared by ionotropic gelation method using chitosan and sodium tripolyphosphate. Total nine batches were formulated as per 3^2 factorial design. Various factors affecting characteristic of nanoparticles were studied.

Table 3.13 Different variables used in chitosan nanoparticle preparation

Independent Variable	Low level (-1)	Medium level (0)	High level (+1)
Conc. of chitosan (X1)	0.1% (w/v)	0.2%(w/v)	0.3% (w/v)
Conc. of NaTPP (X2)	0.25 % (w/v)	0.5% (w/v)	0.75% (w/v)

Table 3.14 Experimental result data with various factors and their responses on formulated batches of chitosan nanoparticles

Batches	Conc. of Chitosan % (w/v)	Conc. of Na TPP % w/v	Particle size (nm)	Zeta Potential (mV)	PDI
1N	0.3	0.75	1044.4± 20.23	+18.89±0.21	0.443

2N	0.2	0.5	716.7± 19.54	+20.19±0.23	0.360
3N	0.1	0.25	381.3±23.56	+22.18±1.02	0.278
4N	0.3	0.25	658.4± 26.77	+28.16±0.87	0.286
5N	0.2	0.75	908.0±15.76	+16.14±0.72	0.364
6N	0.1	0.5	712.9±24.54	+16.56±0.55	0.286
7N	0.3	0.5	740.0±25.87	+22.17±0.32	0.294
8N	0.2	0.25	414.3±27.13	+26.52±0.67	0.296
9N*	0.1	0.75	00	00	00

All the data shown are the mean ± SD (n=3).

 * Batch 9N shown no particles during measurement. It may be due to the minimum zeta potential (very close to zero) that caused settling of particles and failure of formulated batch.

3.5.1 Particle size analysis of formulated chitosan nanoparticles

The ionic interaction between chitosan (positively charged) and TPP (negatively charged) resulted in formation of positively charged chitosan nanoparticles at room temperature. The mean particle size and size distribution of formulated batch were analyzed by Nano plus HD (DLS Analyzer). Particle size and PDI of formulated batches ranged from 414.3 ± 2.71 to 1044 ± 20.23 nm and 0.278 to 0.443 as shown in Table 3.14 and 3.15. The PDI (Polydispersity index) value > 0.5 indicates narrow size distribution of particles. The Particle size of best batch (8N) was found to be 414.3±27.13nm.

Table 3.15 Different Particle size of formulated batches of chitosan nanoparticles

Batches	**Particle size (nm)**
1N	1044.4 ± 20.23

2N	716.7 ± 19.54
3N	381.3 ± 23.56
4N	658.3 ± 26.77
5N	908.0 ± 15.76
6N	712.9 ± 24.54
7N	740.0 ± 25.87
8N	414.3 ± 27.13
9N	00

All the data shown are the mean $\pm$ SD (n=3).

3.5.2 Zeta potential of formulated chitosan nanoparticles

The particle size and surface charge are critical determinants for fate of delivered nanoparticles. Zeta potential is surface charge that greatly affects the particle stability in colloid system through electrostatic repulsion. The particle aggregation is less likely to occur in case of highly charged particles i.e. above ± 30mV. Zeta potential values in all formulated batches ranged between $+14.19 \pm 0.21$to $+28.16 \pm 0.87$ mV. This indicates moderate stability of formulations as shown in Table 3.16. The Positive zeta potential value is due to availability of free NH_3^+. The zeta potential of best batch (8N) was found to be $+26.52 \pm 0.67$ mV.

Table 3.16 Different Zeta Potential of formulated batches of chitosan nanoparticles

Batches	**Zeta Potential (mV)**
1N	$+18.89 \pm 0.21$
2N	$+20.19 \pm 0.23$
3N	$+22.18 \pm 1.02$

4N	+28.16±0.87
5N	+16.14±0.72
6N	+16.56±0.55
7N	+22.17±0.32
8N	+26.52±0.67
9N	00

All the data shown are the mean ± SD (n=3).

3.5.3 SEM (Scanning Electron Microscopy) study of chitosan nanoparticles

The shape and surface morphology of optimized batch (8N) was studied by FE-SEM (scanning electron microscopy). SEM analysis revealed that the use of factorial design resulted particles with target size and narrower size. The particles were found to be spherical in shape with a smooth surface as shown in fig 3.18 (a) & 318 (b)
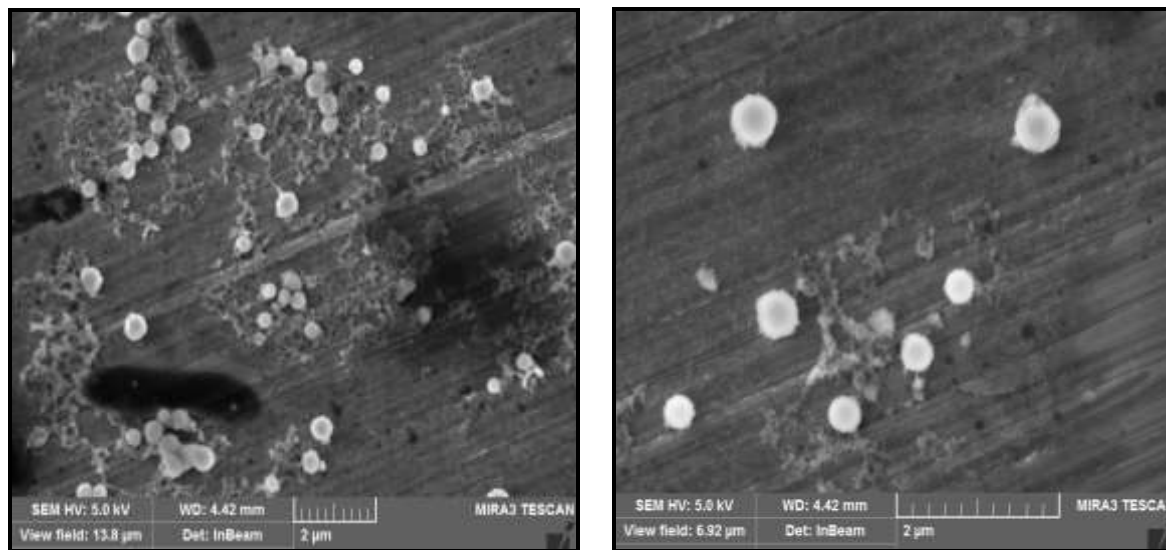
(a)   **(b)**

Fig 3.18 (a) & (b) SEM images of chitosan nanoparticles

3.5.4 Entrapment efficiency and drug loading capacity of chitosan nanoparticles

The entrapment efficiency (%) and drug loading capacity (%) of various batches (1N - 9N) were determined. The results revealed that increase in polymer concentration lead to increase in particle size, entrapment efficiency and drug loading capacity to certain concentration but after that there was no significant increase in entrapment efficiency and drug loading capacity as shown in Table 3.17. The expected reason for this might be that increased concentration of polymer lead to increased viscosity which avoided aggregation of drug in nanoparticles, hence reducing the availability of drug for entrapment. The entrapment efficiency increased up to $56.96 \pm 0.31\%$ and $65.45 \pm 0.023\%$ while drug loading capacity increased up to $16.23 \pm 0.21\%$ and $16.78 \pm 0.76\%$ for INH and PYZ respectively.

Table 3.17 Drug entrapment efficiency and loading capacity of formulated batches of chitosan nanoparticles

Batches	Particle size (nm)	Entrapment efficiency (%)		Drug loading efficiency (%)	
		INH	PYZ	INH	PYZ
3N	381.3 ± 23.56	55.32 ± 0.34	62.15 ± 0.12	11.34 ± 0.23	14.23 ± 0.32
8N	414.3 ± 27.13	55.29 ± 0.06	63.14 ± 0.29	11.99 ± 0.78	14.65 ± 0.24
4N	658.3 ± 26.77	56.13 ± 0.08	64.35 ± 0.35	12.76 ± 0.12	15.32 ± 0.28
6N	712.9 ± 24.54	56.93 ± 0.23	65.13 ± 0.16	14.87 ± 0.54	15.64 ± 0.06
2N	716.7 ± 19.54	56.96 ± 0.31	65.45 ± 0.023	16.23 ± 0.21	16.78 ± 0.67
7N	740.0 ± 25.87	56.0 ± 0.05	64.98 ± 0.15	15.23 ± 0.18	15.89 ± 0.24
5N	908.0 ± 15.76	32.63 ± 0.24	31.13 ± 0.32	6.54 ± 0.054	7.34 ± 0.18
1N	1044.4 ± 20.23	32.04 ± 0.32	29.34 ± 0.01	5.34 ± 0.32	6.21 ± 0.13
9N	00	00	00	00	00

All the data shown are the mean ± SD (n=3).

 * Batch 9N formulation failed

3.5.5 EFFECT OF VARIOUS VARIABLES ON PARTICLE SIZE OF CHITOSAN NANOPARTICLES (CS NPs)

3.5.5.1 Effect of Chitosan concentration on particle size of CS NPs

To study the effect of chitosan concentration on particle size, three set of experiments (3N, 8N, 4N), (6N, 2N, 7N) and (9N, 5N, 1N) were designed. In each set TPP concentration was kept constant but chitosan concentration was varied. Different concentrations of chitosan 1.0, 2.0, 3.0 (mg/ml) in each set, with ratio of 3:1:: CS:TPP (v/v) resulted in formation of nanoparticles. The results revealed that increase in concentration of chitosan lead to increased particle size. It may be due to increased viscosity of inner phases which lead to increased cross linking and increase in particle size.

Table 3.18 Effect of chitosan on particle size of various formulated batches of CS NPs

| SET-I			
Batches	**Chitosan Conc.(mg/ml)**	**Na TPP Conc. (mg/ml)**	**Particle size (nm)**
3N	1.0	2.5	381.3±23.56
8N	2.0	2.5	414.3±27.13
4N	3.0	2.5	658.3± 26.77
SET-II			
Batches	**Chitosan Conc.(mg/ml)**	**Na TPP Conc. (mg/ml)**	**Particle size(nm)**
6N	1.0	5.0	712.9±24.54
2N	2.0	5.0	716.7± 19.54
7N	3.0	5.0	740.0±25.87
SET-III			
Batches	**Chitosan Conc.(mg/ml**	**Na TPP Conc. (mg/ml)**	**Particle size(nm)**
9N	1.0	7.5	00
5N	2.0	7.5	908.0±15.76
1N	3.0	7.5	1044.4± 20.23

All the data shown are the mean ± SD (n=3).
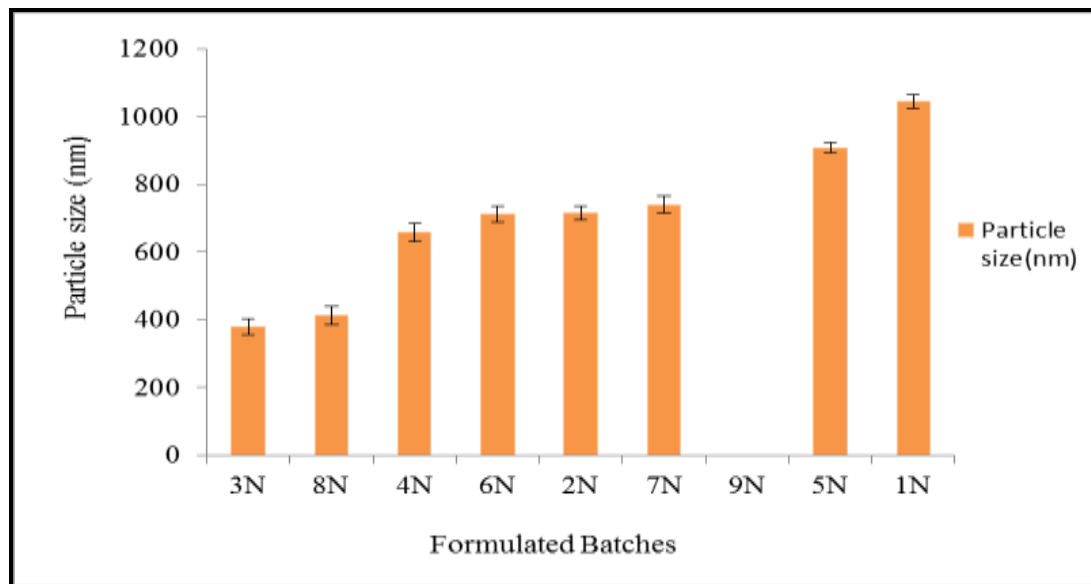
Fig 3.19 Effect of Chitosan concentration on particle size of CS NPs

3.5.5.2 Effect of Tripolyphosphate concentration on particle size of CS NPs

Three sets of experiments (3N, 6N, 9N), (8N, 2N, 5N) and (4N, 7N, 1N) were designed using 3^2 factorial design. The chitosan concentration was kept constant in all batches of each set but varied concentration of TPP 2.5, 5.0,7.5 mg/ml was used in each set. Ratio of 3:1:: CS:TPP (v/v) resulted in formation of chitosan nanoparticles. The results reflect that TPP concentration affects particle size of chitosan nanoparticles. Increase in conc. of TPP resulted into increased particle size as can be depicted from Fig 3.20.

Table 3.19 Effect of TPP on Particle size of various formulated batches of CS NPs

SET-I			
Batches	**Chitosan Conc.(mg/ml)**	**Na TPP Conc. (mg/ml)**	**Particle size (nm)**
3N	1.0	2.5	381.3 ± 23.56
6N	1.0	5.0	712.9 ± 24.54
9N	1.0	7.5	00

SET-II			
Batches	Chitosan Conc.(mg/ml)	Na TPP Conc. (mg/ml)	Particle size(nm)
8N	2.0	2.5	414.3 ± 27.13
2N	2.0	5.0	716.7 ± 19.54
5N	2.0	7.5	908.0 ± 15.76
SET-III			
Batches	Chitosan Conc.(mg/ml)	Na TPP Conc. (mg/ml)	Particle size(nm)
4N	3.0	2.5	658.3 ± 26.77
7N	3.0	5.0	740.0 ± 25.87
1N	3.0	7.5	1044.4 ± 20.23

All the data shown are the mean ± SD (n=3).

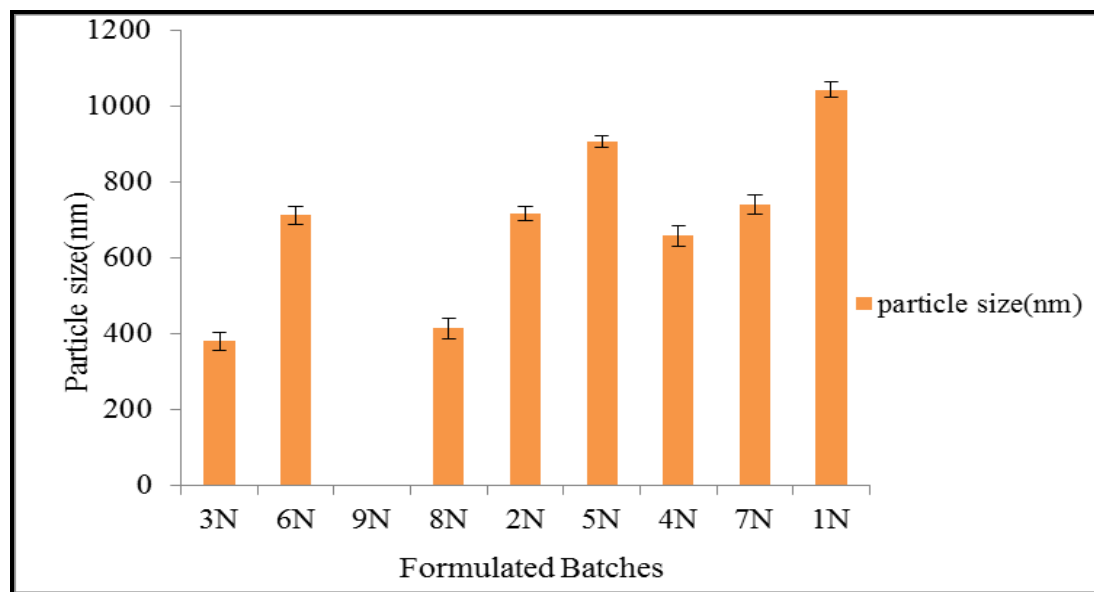**Fig 3.20 Effect of TPP on Particle size of CS NPs**

3.5.6 EFFECT OF VARIOUS VARIABLES ON ZETA POTENTIAL OF CHITOSAN NANOPARTICLES (CS NPs)
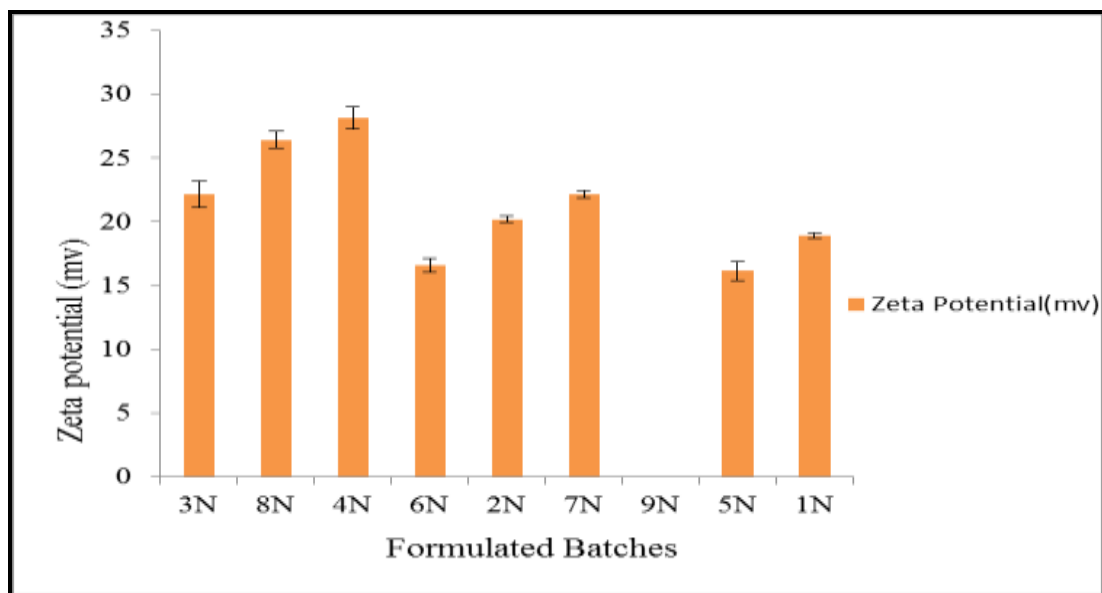
3.5.6.1 Effect of Chitosan concentration on Zeta Potential of CS NPs

The effect of chitosan concentration on zeta potential was studied through three set of experiments (3N, 8N, 4N), (6N, 2N, 7N) and (9N, 5N, 1 N) designed by 3^2 factorial design. The chitosan concentration was varied in each set from 1-3(mg/ml) while TPP concentration was kept constant in all batches of each set as shown in Table 3.20. It is evident from the findings that the zeta potential increased in each set on increasing chitosan concentration from 1-3 mg/ml at fixed TPP. It may be due to increased attribution of NH_3^+ by increased chitosan concentration. The more availability of NH_3^+ by increased chitosan concentration will increase positive value of zeta potential as shown in Fig 3.21.

Table 3.20 Effect of Chitosan on Zeta Potential of various Formulated batches of CS NPs

SET-I			
Batches	**Chitosan Conc.(mg/ml)**	**Na TPP Conc. (mg/ml)**	**Zeta Potential (mV)**
3N	1.0	2.5	+22.18±1.02
8N	2.0	2.5	+26.52±0.67
4N	3.0	2.5	+28.16±0.87
SET-II			
Batches	**Chitosan Conc.(mg/ml)**	**Na TPP Conc. (mg/ml)**	**Zeta Potential (mV)**
6N	1.0	5.0	+16.56±0.55
2N	2.0	5.0	+20.19±0.23
7N	3.0	5.0	+22.17±0.32
SET-III			
Batches	**Chitosan Conc.(mg/ml**	**Na TPP Conc. (mg/ml)**	**Zeta Potential (mV)**
9N	1.0	7.5	00
5N	2.0	7.5	+16.14±0.72
1N	3.0	7.5	+18.89±0.21

All the data shown are the mean ± SD (n=3).

3.21 Effect of Chitosan on zeta potential of CS NPs

3.5.6.2 Effect of Tripolyphosphate concentration on Zeta Potential of CS NPs

The comparative results of zeta potential are shown in fig 3.22. It was performed through three set of experiments (3N, 6N, 9N), (8N, 2N, 5N) and (4N, 7N, 1N). The batches in each set had varied TPP concentration (2.5-7.5mg/ml) while chitosan concentration was kept constant as shown in Table 3.21. It can be depicted from Fig 3.22 that zeta potential of nanoparticles decreased in each set on increasing TPP concentration. The decrease in zeta potential may be due to de-protonation of amine by TPP as a result decrease in positive value of zeta potential.

Table 3.21 Effect of TPP on Zeta Potential of various Formulated batches of Chitosan Nanoparticles.

SET-I			
Batches	Chitosan Conc.(mg/ml)	Na TPP Conc. (mg/ml)	Zeta Potential(mV)
3N	1.0	2.5	+22.18±1.02
6N	1.0	5.0	+16.14±0.72
9N	1.0	7.5	00
SET-II			
Batches	Chitosan Conc.(mg/ml)	Na TPP Conc. (mg/ml)	Zeta Potential(mV)
8N	2.0	2.5	+26.52±0.67
2N	2.0	5.0	+20.19±0.23
5N	2.0	7.5	+16.14±0.72
SET-III			
Batches	Chitosan Conc.(mg/ml	Na TPP Conc. (mg/ml)	Zeta Potential(mV)
4N	3.0	2.5	+28.16±0.87
7N	3.0	5.0	+22.17±0.32
1N	3.0	7.5	+18.89±0.21

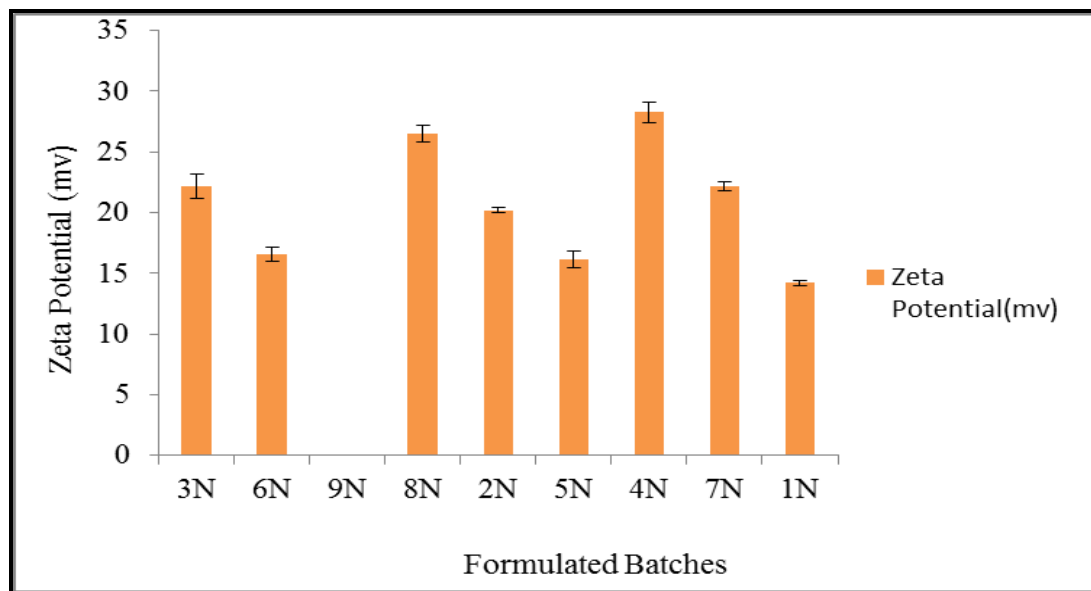All the data shown are the mean ± SD (n=3).

Fig 3.22 Effect of TPP on zeta potential of CS NPs

3.6 *IN-VITRO* DRUG RELEASE STUDY OF CS NPs

The *in vitro* drug release studies of selective batches were carried out in 0.1N HCl (pH 1.2) and phosphate buffer (pH 7.4) using modified diffusion apparatus at 37°C for 2 h and 14 hr respectively. The batches for drug release study were selected on the basis of particle size and zeta potential. *In vitro* release of various batches ranged from 27.66 ±0.88% to 43.97 ± 1.56% and 42.66 ±0.74% to 57.80 ± 1.40 % for INH and PYZ respectively at pH 1.2 (0.1N HCl) for 2h while at pH 7.4 (phosphate buffer) the drug release ranged from 54.39 ± 1.43% to 84.82 ± 2.54% and 61.48 ± 1.52% to 71.24 ± 1.23% for INH and PYZ in 14 h. The optimized batch had showed initial burst release of 20.28% ± 1.43 and 23.62% ± 1.07   followed by controlled release of drug 84.82 ± 2.54 % and 61.48 ± 1.52 % for INH and PYZ respectively at 14 hr. Initial burst release indicates that the drug was localized outwards the nanoparticles. Different release models were applied to determine the best fit model. The release was best explained by zero order as it showed highest regression value (R^2= 0.983 for INH and R^2=0.976 for PYZ). Korsemeyer peppas equation was applied to understand the mechanism of drug release. The release exponent 'n' was 0.374 and 0.281 for INH and PYZ respectively, which indicates zero order release with fickian diffusion.

The *in vitro* release of drug also depends upon particle size. The small size indicates more surface area i.e. more surface area come in contact with medium resulting in faster release. Batch 8N with particle size approx. 414.3 ± 27.13nm showed drug release up to 84.82 ± 2.54% and 61.48 ± 1.52% for INH and PYZ respectively at 14 hr.